Evaluating dynamic multipole polarizabilities and van der Waals dispersion coefficients of two-electron systems with a quantum Monte Carlo calculation: A comparison with some *ab initio* calculations

Michel Caffarel
Laboratoire Dynamique des Interactions Moléculaires, Université Paris VI, Tour 22, 4 place Jussieu, 75252 Paris CEDEX 05, France

Michel Rérat and Claude Pouchan
Laboratoire de Chimie Structurale, Université de Pau, 64000 Pau, France
(Received 14 September 1992)

We present some systematic calculations of dynamic multipole polarizabilities and van der Waals dispersion coefficients for the helium atom and H_2 molecule with a quantum Monte Carlo calculation. Using an original method based on a gauge-invariant formalism we also report some *ab initio* results of the same quantities. In light of the results we discuss the advantages and drawbacks of both approaches in comparison to prior theoretical results.

PACS number(s): 31.20.Di, 31.90.+s

I. INTRODUCTION

Dynamic multipole polarizabilities determine a number of properties of systems interacting with external electric fields. In particular, they can be closely related to the van der Waals dispersion coefficients that describe the long-range interaction of atoms and molecules. It is well known that such quantities which formally involve all the excited states of the system (both the discrete and continuous part of the spectrum) are very difficult to evaluate with accuracy. To illustrate this, it is quite instructive to point out that, for the rather elementary case of the helium atom, it is only in 1976 that Glover and Weinhold [1] were able to determine some high-quality upper and lower bounds of the dynamic dipole polarizabilities; more interestingly, these bounds were tight enough to rule out the majority of previous theoretical and experimental predictions.

A number of approaches based on *ab initio* methods has been devised to obtain dynamic polarizabilities. Among the numerous *ab initio* models currently in use (corresponding to various levels of accuracy) we may cite the self-consistent-field configuration-interaction (SCF-CI) and the full-configuration-interaction (FCI) methods [2–4], the multiconfigurational time-dependent Hartree-Fock or multiconfigurational linear response (MCTDHF and MCLR) [5, 6], the random phase approximation (RPA) [7], or the more elaborate second-order polarization propagator approximation (SOPPA) [8, 9], and a time-dependent gauge-invariant (TDGI) method introducing a dipole-moment factor in the SCF-CI approximation [10–13].

Very recently, Caffarel and Hess have presented a method of computing response properties with quantum Monte Carlo (QMC) [14]. Basically, this scheme relies on the possibility of connecting the imaginary-time-dependent dynamics of the unperturbed system (the time-dependent Green's function closely related to quantum response properties) with the transition probability density of a diffusion process. As a consequence, the usual perturbational components of the Rayleigh-Schrödinger perturbation theory may be expressed in a natural way in terms of stochastic correlation functions of the perturbing potential. These correlation functions are then computed from random walks in configuration space generated using the transition probability density (Langevin techniques). The salient features of this approach will be presented with some detail in Sec. II. It is interesting to note that such a scheme is formally very similar to that of standard molecular dynamics, except that Newtonian trajectories are replaced here by Brownian trajectories (mimicking the "diffuse" character of quantum mechanics).

The chief advantage of the QMC approach with respect to *ab initio* schemes is that no basis-set expansion nor explicit summation over a large, but necessarily incomplete, set of basis functions are introduced. It is, of course, a fundamental property of QMC, considering the importance of such aspects in *ab initio* schemes. Other original features include the possibility of computing several response properties (e.g., dipole, quadrupole, octopole, etc., components) in *one single* Monte Carlo run; the possibility of having a rigorous estimation of the error bars on results (a difficult task for *ab initio* methods); the very favorable computational aspects of QMC (memory requirements are perfectly bounded—no calculation and storage of huge numbers of bielectronic integrals; the computer codes are short, simple and very well suited for vector and parallel computing), etc. All these aspects will be illustrated in this paper.

The quantum Monte Carlo perturbation formalism has been first applied to the problem of the interaction of two helium atoms at short distances [14]. Some preliminary calculations concerning the dynamic dipole polar-

izability of helium have also been reported [15]. In this paper we are concerned with the presentation of some more systematic calculations of dynamic multipole polarizabilities and van der Waals dispersion coefficients for the helium atom and H_2 molecule. These results are presented together with some *ab initio* calculations of the same quantities we performed by using an original formalism based on a TDGI method [12] derived in the spirit of the variation-perturbation approach [16,17] later used by Karplus and Kölker [18] for the time-dependent interaction. The very different features of QMC and *ab initio* approaches are emphasized and the advantages and drawbacks of each of them are discussed in comparison with the most accurate theoretical results available [1,19–41].

Just before completing this work we received a paper from Huiszoon and Briels in which the static dipole polarizabilities of helium and H_2 (at equilibrium geometry) are computed using a differential-diffusion Monte Carlo method [42]. In fact, their approach is very similar to ours as presented in Refs. [14] and [15], and in the present work, except that a branching process is used in their simulations (like in most QMC methods designed so far to compute total energies).

The organization of this paper is as follows. In Sec. II, the quantum Monte Carlo method for computing response properties of two-electron systems is presented. We also give a brief presentation of the TDGI *ab initio* method we shall use for making some comparisons (in particular, when no *ab initio* data are available). Section III presents calculations of dynamic multipole polarizabilities (both in real and imaginary frequencies) for He and H_2. In Sec. IV we present some results concerning van der Waals dispersion coefficients. Finally, some concluding remarks are presented in Sec. V.

II. METHODS

A. Quantum Monte Carlo

Dynamic multipole polarizability components of an N-electron system at frequency ω are given by

$$\alpha_l^{uv}(\omega) = \alpha_l^{uv+}(\omega) + \alpha_l^{uv-}(\omega) \tag{1}$$

with

$$\alpha_l^{uv\pm}(\omega) = \sum_{i\ (\neq 0)} \frac{\langle \phi_0 \mid Q_l^u \mid \phi_i \rangle \langle \phi_i \mid Q_l^v \mid \phi_0 \rangle}{E_i - E_0 \pm \omega}, \tag{2}$$

where Q_l^u stands for the multipole operator:

$$Q_l^u = \left(\frac{4\pi}{2l+1}\right)^{1/2} \sum_i \mid \mathbf{r_i} \mid^l \ Y_l^u(\theta_i, \phi_i), \quad u = -l, \cdots, +l$$

and ϕ_i are the eigenfunctions of H (the Hamiltonian describing the isolated atomic or molecular system) with the corresponding energies E_i. It is easy to see that $\alpha_l^{uv\pm}(\omega)$ may be rewritten in terms of the Laplace transform of the following centered two- (imaginary) time correlation function:

$$\alpha_l^{uv\mp}(\omega) = -\int_0^{+\infty} d\tau\, e^{\pm\tau\omega} \bar{C}_{Q_l^u Q_l^v}(\tau), \tag{3}$$

where

$$\bar{C}_{Q_l^u Q_l^v}(\tau) \equiv \langle \phi_0 \mid (Q_l^u - \bar{Q}_l^u) e^{-\tau(H-E_0)} (Q_l^v - \bar{Q}_l^v) \mid \phi_0 \rangle, \tag{4}$$

and

$$\bar{Q}_l^w \equiv \langle \phi_0 \mid Q_l^w \mid \phi_0 \rangle, \quad w = u, v. \tag{5}$$

The important point is that such correlation functions may be computed by using simulation techniques based on diffusion processes. To do that, we introduce a Markovian diffusion process in configuration space whose transition probability density is closely related to the imaginary-time-dependent Green's function associated with H. More precisely, the transition probability density employed here is

$$p(\mathbf{R} \to \mathbf{R}', t) = \frac{\phi_0(\mathbf{R}')}{\phi_0(\mathbf{R})} \sum_i \phi_i(\mathbf{R}) \phi_i(\mathbf{R}') e^{-t(E_i - E_0)}, \tag{6}$$

where $\mathbf{R}$ is a compact notation for representing a point in the $3N$-dimensional configuration space, that is $\mathbf{R} = (\mathbf{r}_1, ..., \mathbf{r}_N)$, where N is the number of particles of the system. It should be noted that the stationary density, $p(\mathbf{R})$, of the diffusion process (obtained by letting t go to infinity in the preceding formula) is nothing but the usual quantum-mechanical probability density associated with the ground-state wave function

$$p(\mathbf{R}) = \phi_0^2. \tag{7}$$

In practice, a Gaussian short-time version of the transition probability density (6) is used to generate stochastic trajectories of the diffusion process:

$$p(\mathbf{R} \to \mathbf{R}', \Delta t) = \left(\frac{1}{2\pi\Delta t}\right)^{3N/2} e^{-[\mathbf{R}' - \mathbf{R} - \mathbf{b}(\mathbf{R})\Delta t]^2/2\Delta t}, \tag{8}$$

where the so-called drift vector $\mathbf{b}$ responsible for importance sampling is given by

$$\mathbf{b}(\mathbf{R}) = \frac{\boldsymbol{\nabla}\phi_0}{\phi_0}. \tag{9}$$

The effect of drifting the mean value of the Gaussian function (8) is to increase the efficiency of the simulation by keeping the configurations in important regions of phase space. The two-time correlation functions are formally defined in terms of the stationary and transition probability densities as follows:

$$\begin{aligned} \bar{C}_{Q_l^u Q_l^v}(\tau) &= \langle [Q_l^u(\mathbf{R}(0)) - \bar{Q}_l^u][Q_l^v(\mathbf{R}(\tau)) - \bar{Q}_l^v] \rangle \\ &= \int d\mathbf{R}_0 d\mathbf{R}_1 [Q_l^u(\mathbf{R}_0) - \bar{Q}_l^u] p(\mathbf{R}_0) p(\mathbf{R}_0 \to \mathbf{R}_1, \tau) [Q_l^v(\mathbf{R}_1) - \bar{Q}_l^v], \end{aligned} \tag{10}$$

where $\langle\ \rangle$ denotes the average with respect to stochastic trajectories. The validity of Eq. (10) is easily checked by inserting expressions (6) and (7) into (10) and comparing with (4). In practice, such averages may be calculated from random walks generated from Eqs. (8)–(9) and by averaging the two-time product of Q's along them. However, at this point this scheme is rather formal since the ground-state wave function of H [whose expression is needed to construct the drift vector (9)] is generally not known. In fact, it is possible to avoid this problem by introducing a new diffusion process defined from a known trial wave function ψ_T instead of the exact one [43]. In order to compute the very same correlation functions, it is possible to show that one just has to introduce a suitable weight factor in the preceding averages (for a detailed presentation, see [14] and [43]). For example, the two-time correlation functions in which we are interested here are expressed as

$$\langle[\ Q_l^u(\mathbf{R}(0)) - \bar{Q}_l^u][Q_l^v(\mathbf{R}(\tau)) - \bar{Q}_l^v]\rangle = \lim_{t\to+\infty} \frac{\langle [Q_l^u(\mathbf{R}(0)) - \bar{Q}_l^u][Q_l^v(\mathbf{R}(\tau)) - \bar{Q}_l^v] e^{-\int_{-t/2}^{t/2} E_L(\mathbf{R}(s))ds}\rangle_{\psi_T}}{\langle e^{-\int_{-t/2}^{t/2} E_L(\mathbf{R}(s))ds}\rangle_{\psi_T}}, \tag{11}$$

where averages of the right-hand side of the equation are defined with respect to the diffusion process built from a trial wave function ψ_T. In fact, formula (11) is nothing but a generalization of the well-known Feynman-Kac formula [43]. The quantity E_L appearing in the weight (Feynman-Kac) factor is defined as

$$E_L = H\Psi_T/\Psi_T \tag{12}$$

and is usually referred to as the local energy.

As discussed in length in [14] it is important to emphasize that the formalism presented here is effective for systems having no more than two electrons (no antisymmetry constraints from the Pauli principle). In theory bigger systems could be treated by introducing some projecting weights with appropriate antisymmetry. In practice, doing this introduces a dramatic sign problem at large times which renders the simulation very delicate to perform. Note that the commonly used fixed-node approximation cannot be employed for computing multitime correlation functions (even if the exact nodes of the ground state were known, see [14]). Some proposals to control this difficulty have been very recently proposed by one of us [44, 45]. However, the situation is not yet fully satisfactory.

B. *Ab initio* TDGI method

Since this original *ab initio* method has been described in detail in Ref. [12], only its main features will be given here. The dynamic polarizability components [Eqs. (1)–(2)] may be obtained from a time-dependent variation-perturbation approach [18] using the following expressions:

$$\alpha_l^{uv}(\omega) = -\sum_{\pm}\langle\phi_0 \mid Q_l^u - \bar{Q}_l^u \mid 1^{v\pm}\rangle$$

with

$$(H - E_0 \pm \omega)\mid 1^{v\pm}\rangle = -(Q_l^v - \bar{Q}_l^v) \mid \phi_0\rangle \tag{13}$$

where H is the Hamiltonian of the unperturbed (isolated system), ϕ_0 is its ground-state wave function, E_0 the corresponding energy, and $\mid 1^{v\pm} >$ the first-order perturbational wave function.

We have shown elsewhere [12] that the use of a first-order wave function which combines a polynomial function $\hat{g}(\mathbf{r})$ and both true spectral states ϕ_n and quasi-spectral states ψ_m allows us to reach accurate values for static and dynamic polarizability components. For the case of dipole polarizabilities ($Q_l^u = u$) the expression of this first-order wave function is

$$\mid 1^{v\pm}\rangle = \hat{g}^{v^\pm}(\mathbf{r})|\phi_0\rangle + \sum_{n\ (>0)}^{N} c_n^{v^\pm}|\phi_n\rangle + \sum_m^M c_m^{v^\pm}|\psi_m\rangle, \tag{14}$$

where $\hat{g}(\mathbf{r})$ is a first degree polynomial function of the electronic coordinate:

$$\hat{g}^{v^\pm}(\mathbf{r}) = \sum_u a_u^{v^\pm} u \quad \text{with} \quad u, v = x, y, z$$

when the electric field lies in the v direction. ϕ_n are the true spectral states built from Slater determinants

$$\phi_n = \sum_m C_m^n \psi_m,$$

and ψ_m is a quasispectral series determined by Slater determinants selected using the following threshold:

$$s = \left|\frac{q\langle\phi_0|v|\psi_m\rangle}{H_{mm} - E_0}\right|$$

with $H_{mm} = \langle\psi_m|H|\psi_m\rangle$.

The computation of the dynamic polarizability requires the calculations of $a_u^{v^\pm}$, $c_n^{v^\pm}$, and $c_m^{v^\pm}$ factors obtained by projecting Eqs. (13) (for $+\omega$ and $-\omega$) on $v|\phi_0\rangle$, $|\phi_n\rangle$, and $|\psi_m\rangle$. This leads to a system of two linear sets of equations to be solved.

When the origin is fixed at the electronic centroid, the dynamic dipole polarizability components are given in atomic units by

$$\alpha_{l=1}^{uv}(\omega) = \sum_{\pm,w} a_w^{v\pm} \langle wu \rangle + \sum_{\pm,n} c_n^{v\pm} \langle \phi_0 | u | \phi_n \rangle + \sum_{\pm,m} c_m^{v\pm} \langle \phi_0 | u | \psi_m \rangle \quad (15)$$

with $u, v, w = x, y, z$ and $\langle wu \rangle = \langle \phi_0 | \sum_{i,j}^{n_e} w_i u_j | \phi_0 \rangle$ (n_e being the number of electrons).

We have reformulated the TDGI expressions for the imaginary frequency-dependent dipole polarizability $\alpha(i\omega)$ in order to calculate the dispersion coefficients via the Casimir-Polder formula [46]. The two systems of linear equations become identical but twice greater than for real frequencies. The resolution is made as described by Koch and Harrison [47].

Quadrupole polarizability components are obtained in the same way by replacing the dipole moment operator by the quadrupole moment but the polynomial function $\hat{g}(\mathbf{r})$ has not been used in this case.

III. DYNAMIC MULTIPOLE POLARIZABILITIES FOR HE AND H_2

A. He

Tables I–IV present the dynamic dipole, quadrupole, and octopole polarizabilities of helium as calculated by QMC and TDGI (present work), and various *ab initio* methods for comparison. The most commonly used method for evaluating dynamic polarizabilities is certainly the time-dependent Hartree-Fock method (TDHF). TDHF results may be largely improved by using a MCSCF wave function as reference (MCTDHF) instead of a single one [25]. However, for a simple two-electron system such as He nearly exact results may be obtained using full CI (FCI) calculations or explicitly correlated wave functions [1, 24, 37]. Note also that, in the case of He, Glover and Weinhold [1] have used a method for calculating rigorous upper and lower bounds to dynamic dipole polarizabilities using explicitly correlated wave functions. To study the reliability of QMC and TDGI methods, our values are to be compared to these almost exact results when possible.

Let us first discuss the QMC results. As emphasized in Sec. II A a central role is played by the trial wave function used. The closer the exact solution of the trial wave function is, the smaller the fluctuations of the local energy (12) are, and the better the simulation for a given amount of computer time is. In practice, one of the best trial wave functions available for the system under consideration is generally chosen. The wave function may have a rather arbitrary form since only its first (drift vector) and second derivatives (local energy) are to be calculated (no integrals to perform). Highly and explicitly correlated trial wave functions (i.e., including the interelectronic distance) are generally used. Here, we have chosen a rather simple form

$$\Psi_T = |1s(r_1)\rangle |1s(r_2)\rangle \exp\left(\frac{a r_{12}}{1 + b r_{12}}\right) \quad (16)$$

with

$$|1s(r)\rangle = \sum_{i=1}^{3} c_i \exp(-\lambda_i r),$$

where parameters a, b, λ_i, and c_i have been optimized to minimize the energy. With our optimized trial wave function ($a = 0.5$; $b = 0.515\,71$; c_1=0.006 98; c_2=0.367 14; c_3=0.537 62; λ_1=4.462; λ_2=2.8955; λ_3=1.5689) we re-

TABLE I. Dynamic dipole polarizabilities $\alpha(\omega)$ (in a.u.) of He for real frequencies (in a.u.). GW stands for Glover and Weinhold [1], QMC for quantum Monte Carlo, and TDGI, TDHF [25], MCTDHF or MCLR [25], SOPPA [27], and FCI [26] for the corresponding *ab initio* methods. Statistical errors on the last digit of QMC results are indicated in parentheses.

Frequency ω	$\alpha(\omega)$						
	QMC	TDGI	GW	TDHF	MCLR	SOPPA	FCI
0.00	1.382(16)[a]	1.3827	1.3834(8)	1.3214	1.3821	1.3674	1.3846
0.05	1.386(17)		1.3872(8)			1.3712	1.3885
0.10	1.398(17)	1.3984	1.3990(8)	1.3354	1.3976	1.3826	1.4003
0.15	1.418(19)		1.4191(8)			1.4022	
0.20	1.449(22)	1.4478	1.4485(8)	1.3797	1.4467	1.4307	1.4500
0.25	1.490(25)		1.4885(9)			1.4695	
0.30	1.546(31)	1.5404	1.5412(9)	1.4619	1.5385	1.5205	1.5431
0.35	1.618(39)		1.6096(10)			1.5866	
0.40	1.715(52)	1.6974	1.6983(11)	1.5995	1.6938	1.6722	1.7009
0.45	1.846(73)		1.8145(13)			1.7840	
0.50	2.031(111)	1.9696	1.9705(15)	1.8327	1.9621	1.9334	1.9746
0.55	2.318(188)		2.1875(18)		2.1753	2.1402	
0.60	2.858(399)	2.5091	2.5091(23)	2.2741	2.4897	2.4441	
0.65			3.0391(34)			2.9380	
0.70		4.1308	4.1184(73)	3.4320	4.0339	3.9173	4.1527
0.75			8.1640(761)				

[a]Reference [42]: $\alpha(0)$=1.38(1).

cover 89% of the correlation energy. Stochastic trajectories in the six-dimensional configuration space are generated using the Gaussian transition probability density (8) with

$$\mathbf{b}(\mathbf{R}) = \frac{\boldsymbol{\nabla}\Psi_T}{\Psi_T}. \tag{17}$$

As usual when using a step-wise procedure to generate trajectories, a finite time-step error is introduced (the "short-time error"). In order to reduce it significantly we have used the acceptance-rejection procedure presented in Refs. [14] and [48], essentially a standard Metropolis algorithm based on a Langevin move. To keep the short-time error under control, we have repeated our simulations for different time steps of decreasing magnitude up to some value for which the time-step error is significantly smaller than the statistical one. A typical value of the time step for the simulations presented here is 0.01 a.u. The following autocorrelation functions have been calculated:

$$C_l(\tau) = \langle (Q_l - \bar{Q}_l)(0)(Q_l - \bar{Q}_l)(\tau)\rangle, \quad l = 1,2,3 \tag{18}$$

TABLE II. Dynamic dipole polarizabilities $\alpha(\omega)$ (in a.u.) of He for imaginary frequencies (in a.u.). GW stands for Glover and Weinhold [20], QMC for quantum Monte Carlo, and TDGI for the *ab initio* method. Statistical errors on the last digit of QMC results are indicated in parentheses.

Frequency ω	$\alpha(i\omega)$		
	QMC	TDGI	GW
0.00	1.382(16)[a]	1.3827	1.3834(8)
0.05	1.378(16)		
0.10	1.366(15)	1.3675	1.370(10)
0.15	1.347(14)		
0.20	1.322(12)	1.3242	1.322(7)
0.25	1.291(11)		
0.30	1.256(9)	1.2587	1.257(5)
0.35	1.217(7)		
0.40	1.175(6)	1.1788	1.178(4)
0.45	1.132(5)		
0.50	1.088(4)	1.0918	1.090(3)
0.55	1.044(4)		
0.60	1.001(4)	1.0035	1.002(2)
0.65	0.958(4)		
0.70	0.916(4)	0.9180	0.917(2)
0.75	0.875(4)		
0.80	0.836(4)	0.8377	0.836(2)
0.85	0.799(4)		
0.90	0.763(4)	0.7637	0.762(2)
0.95	0.729(4)		
1.00	0.696(3)	0.6964	0.695(2)
1.10	0.635(3)	0.6358	
1.20	0.581(3)	0.5813	0.580(1)
1.30	0.532(2)	0.5326	
1.40	0.488(2)	0.4891	
1.50	0.449(1)	0.4501	0.449(1)
2.00	0.305(1)	0.3075	0.3069(9)
3.00	0.1647(7)	0.1659	
4.00	0.1016(3)		
5.00	0.0686(1.5)		

[a]Reference [42]: $\alpha(0)$=1.38(1).

where the Q_l's are the dipole ($l = 1$), quadrupole ($l = 2$), and octopole ($l = 3$) operators given by (only one component for each multipole moment has been considered because of spherical symmetry)

$$Q_1 = x_1 + x_2,$$
$$Q_2 = \tfrac{3}{2}(x_1^2 + x_2^2) - \tfrac{1}{2}(r_1^2 + r_2^2),$$
$$Q_3 = x_1^3 + x_2^3 - \tfrac{3}{2}x_1(y_1^2 + z_1^2) - \tfrac{3}{2}x_2(y_2^2 + z_2^2),$$

where x_i, y_i, z_i denotes the position of electron i. A very important feature of this type of approach is that the different correlation functions are computed from a *common* set of random walks. Only integrands change when computing different averages. It should be noted that within the framework of *ab initio* methods computing polarizabilities corresponding to different multipole moments requires in theory as many calculations as different operators. In practice, this is not strictly true (the perturbation-independent part of the calculation is evaluated only once; it is possible to take advantage of efficient algorithms for solving simultaneous equations, etc.), but the cost remains larger. Figure 1(a) (upper curve) presents the dipole correlation function C_1 versus τ as calculated for several statistically independent sets of random walks (here, only eight curves have been drawn). The location of the different curves gives a visual representation of the dispersion of QMC results. The number of independent calculations done for any result presented in this paper is always of the order of 100, the error bars given in the tables being estimated from these statistically independent sets of trajectories. As usual when computing correlation functions it is important to realize that the long-time regime may be difficult to reproduce. The reason for that is the exponential decay of the function, together with the presence of an error bar more or less constant as a function of time. We illustrate this difficulty by showing the logarithm of $C(\tau)$ in Fig. 1(b) (lower curve). The theoretical expression (4) indicates that lnC should become linear for sufficiently large times (the slope representing the gap in energy of the system). In practice, this is what happens for large enough times (here, around $\tau \approx 2$ a.u.); however, at too large times (here, around $\tau > 3$ a.u.) the noise dominates. To compute polarizabilities and van der Waals force constants [Eqs. (3) and (22)] the correlation function must be integrated over the entire time domain. Therefore, we must pay special attention to the long-time domain. The strategy employed here is simple. We determine at large times a range of time values where the correlation function decays as a single exponential and for which the noise is still small. On this interval a fit of the correlation function as a single exponential is performed. This representation for $C(\tau)$ is used for ulterior times. In the short-time regime, the data are represented analytically via a spline interpolation procedure. Accordingly, the integrations involved in (3) and (22) are expressed as a finite sum (the number of QMC points) of Laplace transforms of a third-order polynomial (spline part) plus a trivial residue corresponding to large times. Here also, as in the case of evaluating properties related to different multipole op-

erators, it is important to stress that we do not need to do two separate calculations when both imaginary- and real-frequency polarizabilities are needed. Indeed, once the multipole correlation function has been computed as a function of time over a sufficiently large range of time values, evaluating multipole polarizabilities at zero or arbitrary frequencies (real or imaginary) and even van der Waals dispersion coefficients is just a matter of performing a few trivial analytical integrations. Let us now have a closer look at our QMC results. A first observation is that the results obtained are good since in all cases (Tables I–IV) they are compatible with the estimated exact values. This is, of course, expected since QMC results are supposed to be exact and free of any systematic error (such as the choice of the basis set in *ab initio* methods). The only relevant quantity here is the magnitude of the error bar defining the accuracy of the QMC simulation. According to the central-limit theorem, the error bar behaves as $c/\sqrt{T}$, where T is the computer CPU time which is directly related to the total number of Monte Carlo steps performed. c is a constant depending on different factors such as the quality of the trial wave function used and the amount of statistical correlation between successive configurations generated and the nature of the operators involved in the averages. Since in the present work a common set of trajectories has been used to compute all the quantities presented, differences in statistical errors are mainly due to the nature of operators. In particular, it is worth noting that the statistical error on polarizabilities increases when multipole operators corresponding to increasing l are considered. To explain this we first notice that errors on polarizabilities and correlation functions are expected to be roughly proportional due to the linear relation between them. On the other hand, a rough estimate of the error on correlation functions may be obtained by evaluating this error at the initial time, which is essentially given by the dispersion of the squared multipole operator. We have

$$\frac{\delta\alpha_l}{\alpha_l} \sim \frac{\delta C(0)}{C(0)} \sim \frac{\sqrt{\langle\phi_0 \mid \delta Q_l{}^4 \mid \phi_0\rangle - \langle\phi_0 \mid \delta Q_l{}^2 \mid \phi_0\rangle^2}}{\langle\phi_0 \mid \delta Q_l{}^2 \mid \phi_0\rangle}, \tag{19}$$

where

$$\delta Q_l \equiv Q_l - \bar{Q}_l.$$

A crude estimate of these errors may be obtained by com-

TABLE III. Dynamic quadrupole polarizabilities (in a.u.) of He for both real and imaginary frequencies (in a.u.). BL stands for Bishop and Lam [24]. Statistical errors on the last digit of QMC results are indicated in parentheses.

Frequency ω	$C(\omega)_{\mathrm{QMC}}$	$C(\omega)_{\mathrm{TDGI}}$	$C(\omega)_{\mathrm{BL}}$	$C(i\omega)_{\mathrm{QMC}}$	$C(i\omega)_{\mathrm{TDGI}}$
0.00	0.800(16)	0.8022	0.8146	0.800(16)	0.8022
0.05	0.802(16)		0.8161	0.799(16)	
0.10	0.807(16)	0.8085	0.8208	0.794(15)	0.7960
0.15	0.815(17)		0.8289	0.787(15)	
0.20	0.827(17)	0.8280	0.8404	0.776(15)	0.7781
0.25	0.843(18)		0.8559	0.763(14)	
0.30	0.864(20)	0.8633	0.8757	0.749(13)	0.7504
0.35	0.891(22)		0.9007	0.732(13)	
0.40	0.926(26)	0.9192	0.9318	0.714(12)	0.7153
0.45	0.972(31)		0.9705	0.695(11)	
0.50	1.034(40)	1.0058	1.0189	0.675(10)	0.6754
0.55	1.125(57)		1.0802	0.655(10)	
0.60	1.287(104)	1.1449	1.1596	0.634(9)	0.6331
0.65			1.2661	0.613(9)	
0.70		1.3965	1.4172	0.593(8)	0.5903
0.75			1.6541	0.572(8)	
0.80		2.0946		0.552(7)	0.5485
0.85				0.533(7)	
0.90				0.513(6)	0.5086
0.95				0.495(6)	
1.00				0.477(6)	0.4712
1.10				0.442(5)	0.4364
1.20				0.410(5)	0.4043
1.30				0.381(4)	0.3750
1.40				0.353(4)	0.3482
1.50				0.329(4)	0.3237
2.00				0.233(2)	0.2301
3.00				0.129(1)	0.1296
4.00				0.0803(3)	
5.00				0.0545(2)	

puting the averages in (19) using the approximate trial wave function instead of the exact one. Resorting to a standard Metropolis algorithm to compute integrals we obtain

$$\frac{\delta\alpha_2}{\alpha_2}\Big/\frac{\delta\alpha_1}{\alpha_1} \sim 2.5,$$
$$\frac{\delta\alpha_3}{\alpha_3}\Big/\frac{\delta\alpha_1}{\alpha_1} \sim 6.8.$$

These ratios agree quite well with ratios of QMC errors presented in Tables I–IV. For the case of the dipole results, our values are compatible with the narrow range of possible values resulting from the very tight rigorous upper and lower bounds of Glover and Weinhold [1, 20] obtained by using correlated Hylleraas-type wave functions or, for the static case, with the experimental value of 1.383 79(7) obtained by Gugan and Michel [49] [after correcting for the motion of the nucleus we get 1.383 23(7), in agreement with the best *ab initio* value (1.383 192) given by Bishop and Lam [24]].

This is true for both real and imaginary frequencies. Concerning quadrupole polarizabilities our results are compatible with our TDGI results and the results obtained by Bishop and Lam [24] (note that we have divided our results by a factor 3 to match their convention). Table IV presents dynamic octopole polarizabilities of He. They are compared with the *ab initio* results of Luyckx, Coulon, and Lekkerkerker [38] obtained by a simple variation method. The latter ones agree quite well with our QMC results within statistical errors. Another feature which deserves to be commented on is the increase of the statistical error with real frequency. This behavior arises from the fact that high real frequencies require an accurate evaluation of the correlation function for increasing times [the Laplace kernel $\exp(\omega\tau)$ in (3) explodes for large frequencies], and the small statistical errors on the tail of the correlation function are then exponentially magnified by the Laplace transform. Note that this problem does not exist in the case of imaginary frequencies.

In order to make some comparisons, a number of *ab initio* calculations are also presented in Tables I–IV. Our *ab initio* calculations were performed using the TDGI approach [12, 13] briefly presented in Sec. II B. For He, the basis set employed consists of $13s$, $7p$, and $6d$ primitive Gaussian orbitals based on the van Duijneveldt ($10s$) primitive set [50, 51] and an even tempered ($7p, 6d$) polarization set augmented by adding $3s$ diffuse function.

TABLE IV. Dynamic octopole polarizabilities (in a.u.) of He for both real and imaginary frequencies (in a.u.). *Ab initio* results are taken from Ref. [38]. Statistical errors on the last digit of QMC results are indicated in parentheses.

Frequency ω	$\alpha_3(\omega)_{\mathrm{QMC}}$	$\alpha_3(\omega)_{ab\ initio}$	$\alpha_3(i\omega)_{\mathrm{QMC}}$	$\alpha_3(i\omega)_{ab\ initio}$
0.00	10.36(69)	10.48[a]	10.36(69)	10.48[a]
0.05	10.38(70)	10.49	10.33(69)	10.46
0.10	10.45(71)	10.54	10.26(68)	10.42
0.15	10.57(72)	10.63	10.15(66)	10.34
0.20	10.75(75)	10.74	10.01(64)	10.23
0.25	11.00(80)	10.90	9.83(62)	10.10
0.30	11.33(86)	11.10	9.62(59)	9.94
0.35	11.77(96)	11.34	9.40(57)	9.76
0.40	12.35(113)	11.64	9.16(54)	9.56
0.45	13.14(144)	12.01	8.91(51)	9.35
0.50	14.26(212)	12.45	8.66(49)	9.12
0.55			8.41(46)	8.89
0.60			8.17(44)	8.65
0.65			7.92(41)	8.40
0.70			7.69(39)	8.15
0.75			7.46(36)	7.90
0.80			7.23(34)	7.66
0.85			7.02(32)	7.41
0.90			6.81(30)	7.17
0.95			6.61(28)	6.93
1.00			6.41(26)	6.70
2.00			3.51(9)	3.42
3.00			1.92(2)	1.93
4.00			1.198(9)	1.217
5.00			0.820(11)	0.828
6.00			0.591(8)	0.597
7.00			0.452(4)	0.449
8.00			0.350(3)	0.350
9.00			0.276(3)	0.280
10.0			0.225(2)	0.228

[a]Reference [37]: $\alpha_3(0) = 10.6144$.

Exponents of the $3s$ orbitals are, respectively, 0.049 069, 0.022 304, and 0.010 138. SCF and CI calculations within this basis set give an atomic energy of $-2.861\,67$ a.u. and $-2.902\,52$ a.u., respectively. Dynamic dipole polarizabilities of He for real frequencies computed with TDGI are listed in Table I together with some TDHF [25], MCLR [25], SOPPA [27], and FCI [26] results and the very accurate rigorous upper and lower bounds obtained by Glover and Weinhold [19, 20]. A first point to emphasize is that our *ab initio* TDGI results for the static polarizability (1.3827 a.u.) is in excellent agreement with the one obtained by Glover and Weinhold [1.3834(8)] and with the very accurate value (1.383 192) given by Bishop and Lam [24] using explicitly electron-correlated wave functions.

MCTDHF and FCI methods give quite accurate results; an error of approximately 1% is found with SOPPA. The main differences between various calculations appear at frequencies close to the first excitation energy of He. Table I shows that, for frequencies up to 0.7 a.u., the TDGI results, close to the accurate results of Glover and Weinhold [1], are the most accurate ones among *ab initio* calculations. The main explanation is that the excitation energy corresponding to the transition $1s \rightarrow 2p$ is very well reproduced in our calculations, namely, 21.193 eV, to be compared with the experimental value of 21.22 eV. As already explained above QMC results have a statistical error which increases very rapidly with the frequency. Calculating polarizabilities for real frequencies close to the excitation energy is not an easy task for the QMC approach. For the case of imaginary frequencies where this problem does not exist, we obtain a very good agreement between QMC and TDGI results (Table II). Concerning the dynamic quadrupole polarizabilities (Table III) our results are compared with those obtained by Bishop and Lam [24] which have to be considered as reference values. Between 0.0 and 0.6 a.u. our *ab initio* values have a similar behavior as Bishop and Lam results. However, it seems that our results are too

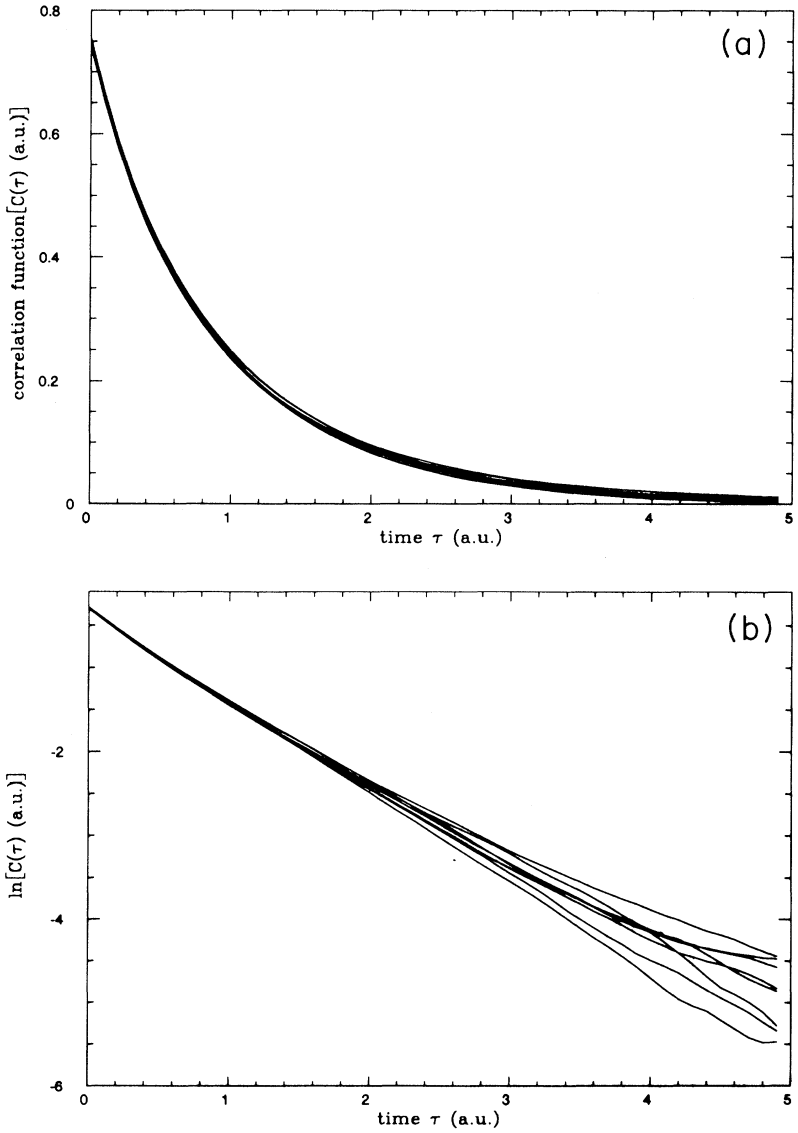

FIG. 1. (a) Dipole correlation functon of He vs τ as calculated in eight independent runs. (b) Logarithm of $C(\tau)$. Note the effect of the noise in the large-time domain.

small with an error of approximately 1.5%. QMC results within the statistical errors are in good agreement with both sets of results.

B. H_2

Calculating response properties for a molecular system such as H_2 using QMC does not introduce any additional difficulties with respect to an atomic system such as He. As usual choosing a good approximate trial wave function is the crucial step. Since calculations at both intermediate and large internuclear separations, $R_{\text{H-H}}$, are considered here it is important to choose a wave function capable of describing both the equilibrium region (covalent regime) and the large $R_{\text{H-H}}$ region (valence-bond regime). This could be realized with one single wave function with some parameters connecting both cases. For simplicity we have chosen here to use two different wave functions

For large distances

$$\Psi_T = \exp\left(\frac{ar_{12}}{1+br_{12}}\right)[\Phi_A(1)\Phi_B(2)+\Phi_A(2)\Phi_B(1)] \tag{20}$$

with

$$\Phi_M(i) = \exp(-\lambda_1 r_{iM}) + c\exp(-\lambda_2 r_{iM}), \quad M = A, B,$$

where r_{iM} denotes the distance between electron i and nucleus M ($M = A, B$).

For intermediate distances

$$\Psi_T = \exp\left(\frac{ar_{12}}{1+br_{12}}\right)\Phi(1)\Phi(2), \tag{21}$$

where the molecular orbital is given by

$$\Phi(i) = \exp(-\lambda r_{iA}) + \exp(-\lambda r_{iB}).$$

Concerning our *ab initio* TDGI calculations, we have chosen for each hydrogen atom a contracted basis $[6s, 6p, 3d]$ issued from the basis $[4s, 3p, 1d]$ proposed by Siegbahn and Liu [52] in their study of the potential energy surface of H_3. The two additional s functions

TABLE V. Dynamic dipole polarizabilities (in a.u.) of H_2 at $R = 1.4$ for real and imaginary frequencies (in a.u.). QMC stands for quantum Monte Carlo and TDGI, Rych [28] and SOPPA [27] stand for the corresponding *ab initio* methods. Statistical errors on the last digit of QMC results are indicated in parentheses.

Frequencies	$\alpha_\parallel^{\text{QMC}}$	$\alpha_\parallel^{\text{TDGI}}$	$\alpha_\parallel^{\text{Rych}}$	$\alpha_\parallel^{\text{SOPPA}}$	$\alpha_\perp^{\text{QMC}}$	$\alpha_\perp^{\text{TDGI}}$	$\alpha_\perp^{\text{Rych}}$	$\alpha_\perp^{\text{SOPPA}}$
				Real				
0.0000	6.42(8)[a]	6.4310	6.3873	6.4495	4.53(7)[a]	4.5944	4.5786	4.5676
0.0720	6.55(9)	6.5617	6.5164	6.5812	4.60(7)	4.6725	4.6562	4.6445
0.0834	6.59(9)	6.6077	6.5618	6.6276	4.62(7)	4.6999	4.6834	4.6715
0.1045	6.69(9)	6.7132	6.6659	6.7338	4.68(9)	4.7626	4.7457	4.7331
0.1363	6.90(10)	6.9278	6.8776	6.9501	4.79(9)	4.8892	4.8715	4.8576
0.1535	7.04(10)	7.0756	7.0235	7.0990	4.87(10)	4.9758	4.9576	4.9427
0.1979	7.52(13)	7.5865	7.5256	7.6136	5.13(13)	5.2713	5.2503	5.2328
0.2354	8.09(15)	8.2125	8.1412	8.2437	5.43(18)	5.6257	5.6017	5.5800
0.2500	8.37(17)	8.5226	8.4481	8.5568	5.57(22)	5.7982	5.7738	5.7493
0.3000	9.68(34)	10.0190	9.9160	10.0649		6.6041	6.5713	6.5367
0.3500		12.7855	12.6126	12.8558		7.9877	7.9320	7.8834
0.3748		15.2223	14.9610	15.3084		9.1058	9.0182	8.9633
0.4000		19.4440	18.9847	19.5639		10.8521	10.6930	10.6421
0.4500		61.6664	54.3276	62.0977		20.9387	19.4400	20.0551
				Imaginary				
0.0000	6.42(8)[a]	6.4310			4.53(7)[a]	4.5944		
0.1000	6.19(7)	6.1939			4.40(7)	4.4517		
0.2000	5.59(6)	5.5834			4.05(5)	4.0777		
0.3000	4.82(4)	4.8082			3.58(4)	3.5888		
0.4000	4.05(3)	4.0395			3.09(3)	3.0870		
0.5000	3.36(2)	3.3624			2.63(2)	2.6294		
0.8000	1.96(1)	1.9746			1.63(1)	1.6367		
1.0000	1.423(7)	1.4396			1.220(8)	1.2290		
1.2000	1.073(5)	1.0848			0.942(4)	0.9481		
1.5000	0.743(4)	0.7484			0.670(3)	0.6718		
1.8000	0.542(3)	0.5437			0.499(2)	0.4978		
2.0000	0.448(2)	0.4496			0.417(2)	0.4160		

[a]Reference [42]: $\alpha_\parallel(0) = 6.38(5)$; $\alpha_\perp(0) = 4.60(3)$.

and three p functions have an exponent of (0.028 773 9, 0.012 510 3) and (0.101 818, 0.037 025, 0.013 463 5), respectively. The three exponents of the d functions are 1.202 52, 0.463 925, and 0.081 240 6. Even if this basis set is far from being complete, the introduction of the polynomial in the determination of polarizabilities improves the convergence. Performing a full CI calculation within this basis set leads to an energy of $-1.173\,485$ a.u. at R=1.401 a.u. A most important point when determining the dynamical properties of H_2 is to correctly describe the vertical transition $X\,^1\Sigma_g^+ \rightarrow B\,^1\Sigma_u^+$ and $X\,^1\Sigma_g^+ \rightarrow C\,^1\Pi_u$. Our results for the corresponding excitation energies are 12.73 eV and 13.21 eV, respectively, in excellent agreement with the exact values of 12.76 and 13.22 eV.

Table V presents dynamic dipole polarizabilities of H_2 at the equilibrium geometry for both real and imaginary frequencies as computed with QMC and TDGI. Results for real frequencies are compared with the reference calculations by Rychlewski [28] based on a variation-perturbation method using explicitly correlated wave functions and some recent SOPPA results by Sauer, Dierksen, and Oddershede [27].

QMC results for real frequencies are compatible with Rychlewski's values within statistical error bars. Concerning *ab initio* (TDGI) results, it is noted that the static components $\alpha_{zz}(0)$ and $\alpha_{xx}(0)$ overestimate Rychlewski results by a factor of 0.7% and 0.3%, respectively. This overestimation is true for all frequencies. At frequency 0.4 a.u., close to the resonance, our values are too large by a factor of 2.4% and 1.5%, respectively. It should be emphasized that our TDGI results, obtained using a much smaller basis set than Sauer, Dierksen, and Oddershede [27] with SOPPA are of comparable quality. Although the parallel component is better reproduced with TDGI than with SOPPA, this is no longer true for the perpendicular one much more sensitive to the angular correlation. In the case of imaginary frequencies, only our QMC and TDGI results can be compared. Both sets of results appear to be compatible.

Table VI presents dynamic quadrupole polarizabilities of H_2 at the equilibrium geometry for both real and imaginary frequencies for the three independent components denoted as $C_{zz,zz}$, $C_{xz,xz}$, and $C_{xx,xx}$ (z is the internuclear axis), as computed by QMC and TDGI. Our static components and values at real frequency ω=0.0720 a.u. are compatible with those available in the literature [33, 34]. TDGI results are in good agreement with QMC

TABLE VI. Dynamic quadrupole polarizabilities (in a.u.) of H_2 at $R = 1.4$ a.u. for real and imaginary frequencies (in a.u.). QMC and TDGI stand for quantum Monte Carlo and *ab initio*, respectively. Statistical errors on the last digit of QMC results are indicated in parentheses.

Frequencies	$C_{zz,zz}^{\mathrm{QMC}}$	$C_{zz,zz}^{\mathrm{TDGI}}$	$C_{xz,xz}^{\mathrm{QMC}}$	$C_{xz,xz}^{\mathrm{TDGI}}$	$C_{xx,xx}^{\mathrm{QMC}}$	$C_{xx,xx}^{\mathrm{TDGI}}$
			Real			
0.0000[a]	6.10(35)	5.9914	4.30(36)	4.1976	4.93(24)	4.7929
0.0720[b]	6.17(36)	6.0645	4.35(37)	4.2440	4.99(25)	4.8465
0.0834	6.19(38)	6.0879	4.37(38)	4.2601	5.01(26)	4.8651
0.1045	6.25(39)	6.1410	4.40(40)	4.2968	5.05(27)	4.9074
0.1363	6.36(44)	6.2466	4.47(45)	4.3696	5.14(30)	4.9914
0.1535	6.43(47)	6.3177	4.52(49)	4.4186	5.20(32)	5.0478
0.1979	6.66(62)	6.5530	4.68(65)	4.5806	5.41(41)	5.2340
0.2354	6.93(80)	6.8209	4.87(83)	4.7650	5.64(54)	5.4451
0.2500	7.06(90)	6.9461	4.96(93)	4.8511	5.75(62)	5.5433
0.3000		7.4885		5.2236	6.23(115)	5.9652
0.3500		8.2798		5.7656		6.5684
0.3748		8.8137		6.1304		6.9660
0.4000		9.5016		6.5989		7.4656
0.4500		11.6312		8.0344		8.9104
			Imaginary			
0.0000	6.10(35)	5.9914	4.30(36)	4.1976	4.93(24)	4.7929
0.1000	5.98(31)	5.8662	4.21(30)	4.1113	4.82(21)	4.6929
0.2000	5.64(25)	5.5243	3.99(27)	3.8750	4.53(15)	4.4191
0.3000	5.16(18)	5.0444	3.66(19)	3.5428	4.13(11)	4.0336
0.4000	4.63(14)	4.5098	3.29(16)	3.1720	3.69(9)	3.6035
0.5000	4.10(12)	3.9815	2.92(13)	2.8047	3.26(8)	3.1789
0.8000	2.80(9)	2.6840	2.01(9)	1.8986	2.23(5)	2.1454
1.0000	2.18(6)	2.0839	1.59(6)	1.4774	1.75(3)	1.6734
1.2000	1.73(4)	1.6455	1.28(5)	1.1687	1.39(3)	1.3302
1.5000	1.25(2)	1.1935	0.92(2)	0.8495	1.01(1)	0.9760
1.8000	0.921(8)	0.8975	0.680(9)	0.6399	0.768(6)	0.7421
2.0000	0.775(6)	0.7553	0.570(7)	0.5389	0.653(4)	0.6286

[a]Reference [34]: $C_{zz,zz} = 5.983$; $C_{xz,xz} = 4.180$; $C_{xx,xx} = 4.927$.
[b]Reference [34]: $C_{zz,zz} = 6.050$, $C_{xz,xz} = 4.226$, $C_{xx,xx} = 4.981$.

TABLE VII. Dipole static polarizabilities (in a.u.) of H_2 at selected internuclear distances R (in a.u.). Rych stands for Rychlewski [29], BL stands for Bishop and Lam [31], QMC stands for quantum Monte Carlo, and TDGI stands for *ab initio*. Statistical errors on the last digit of QMC results are indicated in parentheses.

Distance R	$\alpha_\perp^{\mathrm{QMC}}$	$\alpha_\perp^{\mathrm{TDGI}}$	$\alpha_\perp^{\mathrm{Rych}}$	$\alpha_\perp^{\mathrm{BL}}$	$\alpha_\parallel^{\mathrm{QMC}}$	$\alpha_\parallel^{\mathrm{TDGI}}$	$\alpha_\parallel^{\mathrm{Rych}}$	$\alpha_\parallel^{\mathrm{BL}}$
1.4	4.53(7)[a]	4.5944	4.57856	4.5785	6.42(8)[a]	6.4310	6.38732	6.3875
2.4	7.61(14)	7.6697	7.66049	7.6592	14.57(57)	14.2932	14.26621	14.2691
3.0	8.76(20)	8.8494	8.85806	8.8555	17.60(79)	17.8692	17.79965	17.9990
3.4	9.01(26)	9.2238	9.22883		18.35(90)	18.3724	18.28339	
3.8	9.13(18)	9.3003	9.30201		17.41(53)	17.3388	17.30680	
4.4	9.10(17)	9.2143			14.59(28)	14.7043		
6.0	8.98(13)	8.9371	8.92719		10.17(17)	10.2007	10.19754	

[a]Reference [42]: $\alpha_\parallel(0) = 6.38(5)$; $\alpha_\perp(0) = 4.60(3)$.

ones, except at large imaginary frequencies where TDGI seems to give too small values.

The dependence of static dipole polarizabilities on the internuclear distance H-H is presented in Table VII. For all distances the TDGI results are in excellent agreement with the reference values obtained by Rychlewski [29]. The same remark is valid for QMC results.

IV. van der WAALS COEFFICIENTS FOR He AND H_2

The multipole dispersion force coefficients between two systems a and b may be expressed in terms of the dynamic polarizabilities as follows (see, e.g., Ref. [53])

$$C^{ab}(l_a, l_b) = \frac{(2l_a + 2l_b)!}{2\pi(2l_a)!(2l_b)!} \int_0^{+\infty} d\omega\, \alpha_{l_a}^a(i\omega)\alpha_{l_b}^b(i\omega), \tag{22}$$

usual van der Waals constants being related to these coefficients in the following way:

$$\begin{aligned} C_6^{ab} &= C^{ab}(1,1), \\ C_8^{ab} &= C^{ab}(1,2) + C^{ab}(2,1), \\ C_{10}^{ab} &= C^{ab}(1,3) + C^{ab}(2,2) + C^{ab}(3,1). \end{aligned} \tag{23}$$

A. c_6-c_8 and c_{10} for He

As already pointed out a remarkable feature of QMC is that no additional calculations are needed to compute van der Waals constants once the polarizabilities have been evaluated. Indeed, when computing polarizabilities we built an analytical representation of the correlation function of each multipole operator. Obtaining van der Waals coefficients is then a simple matter of performing the analytic integrations involved in formula (22). Our results for c_6, c_8, and c_{10} are presented in Table VIII together with some other results found in literature [20,27,35–40]. QMC results appear to be quite good.

Our TDGI results are obtained from the values of the polarizabilities at imaginary frequencies using the

TABLE VIII. van der Waals dispersion coefficients (in a.u.) of He. Statistical errors on the last digit are indicated in parentheses.

Method	c_6	c_8	c_{10}
Glover and Weinhold[a]	1.460(6)		
Maeder and Kutzelnigg[b]	1.457	13.90	177.24
Meyer[c]	1.456	13.90	175.4
Thakkar[d]	1.4608	14.1118	183.6
Luyckx, Coulon, and Lekkerkerker[e]	1.458	14.06	182.2
Buckingham and Hibbard[f]	1.4638	14.094	183.47
SOPPA[g]	1.4394		
MCTDHF[h]	1.4608		
Present work:			
QMC	1.454(14)	13.88(22)	177.9(69)
TDGI	1.4593	13.883	

[a]Reference [20].
[b]Reference [35].
[c]Reference [36].
[d]Reference [37].
[e]Reference [38].
[f]Reference [39].
[g]Reference [27].
[h]Reference [40].

TABLE IX. c_6 dispersion force constant (in a.u.) for He-H_2 as a function of the interhydrogen distance R (in a.u.) with quantum Monte Carlo (QMC) and *ab initio* (TDGI) methods. Comparison with the semiempirical results of Matias and Varandas [41], see text.

Method \ R	1.4	2.4	3.0	3.4	3.8	4.4	6.0
			Parallel				
QMC	4.61(4)	7.81(15)	8.75(22)	8.88(29)	8.30(12)	7.46(11)	5.99(5)
TDGI	4.6267	7.8405	8.8621	8.8602	8.4148	7.4756	6.04
Max. Matias	4.6	7.5		8.6	8.4	7.8	6.6
Min. Matias	4.2	6.8		7.6	7.3	6.7	5.7
			Perpendicular				
QMC	3.53(4)	5.05(6)	5.52(8)	5.64(9)	5.68(9)	5.67(8)	5.59(8)
TDGI	3.5579	5.0702	5.5774	5.7275	5.7563	5.7198	5.61
Max. Matias	4.	6.1		6.9	6.9	6.6	6.4
Min. Matias	3.2	5.8		5.4	5.3	5.2	5.0

Casimir-Polder formalism. More precisely, we first solve Eq. (13) in order to get $\alpha(i\omega)$ for a number of imaginary frequencies. Then, we perform a fit of the resulting curve using the oscillator strengths and transition frequencies as fitting parameters. Finally, the coefficient c_6 is obtained from the following expression:

$$c_6 = \frac{3}{2} \sum_{\nu,\mu} \frac{f_\nu^A f_\mu^B}{\omega_\nu^A \omega_\mu^B (\omega_\nu^A + \omega_\mu^B)}$$

using the optimized parameters. Note that the values of the oscillator strengths (f_ν^A, f_μ^B) and transition frequencies $(\omega_\nu^A, \omega_\mu^B)$ calculated at the CI level for the two systems A and B are used as a starting point of our optimization.

The evaluation of the coefficient c_{10} which requires some additional calculations has not been performed. The values obtained for c_6 and c_8 are in excellent agreement with those obtained by QMC and preceding calculations.

B. c_6 for He-H_2

Table IX presents calculations of the c_6 dispersion force constants (both parallel and perpendicular) for the system He-H_2 as a function of the interhydrogen distance $R_{\text{H-H}}$ with quantum Monte Carlo and *ab initio* (TDGI) methods. To our knowledge this is the first from-first-principles calculation of this quantity. We have compared our results with the recent results of Matias and Varandas ([41]) obtained from a number of more or less crude semiempirical approximations. It is very satisfactory to note that our QMC and TDGI results are compatible (within statistical error bars) for any distance. We have given the upper and lower bounds obtained from calculations by Matias and Varandas (denoted as Min and Max). We see that for a number of distances our evaluations are in complete disagreement with their results. This illustrates how semiempirical evaluations can be significantly poor.

V. DISCUSSION

The purpose of this work was to present some systematic calculations of dynamic multipole polarizabilities and van der Waals dispersion coefficients of two-electron systems (He and H_2) with quantum Monte Carlo results. A detailed presentation of the practical implementation of this new approach has been given. We compared our results with a number of previous theoretical results obtained by using various *ab initio* methods. In all cases QMC results are in good agreement with estimated "exact" values within statistical error bars. The typical statistical error on QMC results is of the order of a few percent. This should be considered as satisfactory, even if for simple systems such as He and H_2 more accurate results have been obtained by using explicitly correlated wave functions (particularly for static quantities). However, it should be noted that the accuracy on QMC results could be increased by making longer Monte Carlo runs (that was not the purpose of this work).

We also reported some results obtained using an original *ab initio* method based on a gauge-invariant formalism (TDGI method). It has been illustrated that TDGI results are of comparable quality with the best *ab initio* values, although the size of our basis sets was significantly smaller. This is essentially due to the fact that, besides giving a good description of the ground-state wave function, in TDGI we also give a very good description of the first excited state, an essential step to correctly reproduce the dynamical properties of the system. Having, at our disposal, this accurate *ab initio* method appeared to be essential in checking our QMC calculations in the interesting cases where QMC results entered in conflict with existing theoretical results. That was, in particular,

the case when calculating the c_6 dispersion coefficient for He-H_2, a quantity for which only semiempirical results were known. In addition, presenting QMC results together with *ab initio* results helps us to emphasize the very different features of both approaches.

QMC does not require any expansion on a basis set. Most of the correlation energy is taken into account via the high-quality trial wave function used. The remaining part is recovered using an appropriate weight factor (Feynman-Kac factor) when computing averages. Such a property is remarkable. In some very rough sense, we may view the various *ab initio* methods referred to in the tables as different clever ways of trying to tackle the problem of basis-set convergence. In particular, as emphasized above, our TDGI method is another original way of getting accurate results from a relatively modest basis set. In addition, it should be emphasized that no error bars appear in tables for *ab initio* results. Indeed, computing errors resulting from an incomplete basis set with a given *ab initio* method is by no way an easy task. In sharp contrast, QMC gives a natural and viable estimate (nonbiased statistical estimator) of the error made for a given amount of numerical effort.

Using our QMC framework based on two-time correlation functions enables us to compute during a same run all the response properties corresponding to different multipole operators (real and imaginary polarizabilities for l=1,2,..., van der Waals dispersion coefficients). This is particularly convenient. Within the framework of an *ab initio* calculation, in theory, a calculation is required for each separate quantity (although in practice it is possible to reduce a non-negligble part of the cost). In particular, that was the reason why we did not compute dynamic octopole polarizabilities with TDGI (even if, of course, this is possible).

The computational aspects of QMC are remarkably favorable: the memory requirements are very small (no calculation and storage of bielectonic integrals); the codes are short, simple, and very well suited for vector and parallel processing.

Finally, we would like to end with some of the limitations of QMC. First, as pointed out above, the method is not suitable for computing real dynamic polarizabilities at a frequency close to a resonance. Big error bars in the frequency region close to 0.7 a.u. in Tables I and III–VI illustrate this point. However, this does not occur for imaginary frequencies which are used for computing van der Waals constants. However, the most important limitation of QMC is that the formalism used in this work is limited in practice to two-electron systems (see discussion at the end of Sec II A), systems for which accurate *ab initio* calculations may be performed using explicitly electron-correlated wave functions. Accordingly, it will be possible to consider QMC as a viable alternative to the use of full CI methods only when efficient methods of computing multitime correlation functions for many-electron systems will be available. This will require some more methodological developments.

ACKNOWLEDGMENTS

We would like to thank the "Centre National de la Recherche Scientifique" (CNRS), the "Ministère de l'Education Nationale" (MEN), and the C3NI of the Centre National Universitaire Sud de Calcul (CNUSC) for their support. Laboratoire Dynamique des Interactions Moléculaires is "Unité de Recherche Propre du CNRS No. 271" and Laboratoire de Chimie Structurale is "Unité de Recherche Associée au CNRS No. 474."

[1] R.M. Glover and F. Weinhold, J. Chem. Phys. **65**, 4913 (1976).
[2] E.N. Svendsen and T. Stroyer-Hansen, Theoret. Chim. Acta **45**, 33 (1977).
[3] H.F. Hameka and E.N. Svendsen, Int. J. Quantum Chem. **11**, 129 (1977).
[4] J. Olsen, A.M. Sanchez de Meras, H.J. Aa Jensen, and P. Jorgensen, Chem. Phys. Lett. **154**, 380 (1989).
[5] J. Olsen and P. Jorgensen, J. Chem. Phys. **82**, 3235 (1985).
[6] P. Jorgensen, H.J. Aa Jensen, and J. Olsen, J. Chem. Phys. **89**, 3654 (1988).
[7] H.J. Aa Jensen, H. Koch, P. Jorgensen, and J. Olsen, Chem. Phys. **119**, 297 (1988).
[8] J. Oddershede and E.N. Svendsen, Chem. Phys. **64**, 359 (1982).
[9] J. Oddershede, P. Jorgensen, and D.L. Yeager, Comput. Phys. Rep. **2**, 33 (1984).
[10] M. Rérat, Int. J. Quantum Chem. **36**, 169 (1989).
[11] M. Rérat, C. Pouchan, M. Tadjeddine, J.P. Flament, H.P. Gervais, and G. Berthier, Phys. Rev. A **43**, 5832 (1991).
[12] M. Rérat, M. Mérawa, and C. Pouchan, Phys. Rev. A **45**, 6263 (1992).
[13] M. Rérat, M. Mérawa, and C. Pouchan, Phys. Rev. A **46**, 5471 (1992).
[14] M. Caffarel and O. Hess, Phys. Rev. A **43**, 2139 (1991).
[15] M. Caffarel and O. Hess, in *Advances in Biomolecular Simulations*, AIP Conf. Proc. No. 239 (AIP, New York, 1991), pp. 20–32.
[16] F. Dupont, J. Tillieu, and J. Guy, J. Phys. Rad. **22**, 9 (1961).
[17] H.F. Hameka, Rev. Mod. Phys. **34**, 87 (1962).
[18] M. Karplus and H.J. Kölker, J. Chem. Phys. **38**, 1263 (1963).
[19] R.M. Glover and F. Weinhold, J. Chem. Phys. **66**, 185 (1977).
[20] R.M. Glover and F. Weinhold, J. Chem. Phys. **66**, 191 (1977).
[21] M. Jaszunski and R. McWeeny, Mol. Phys. **46**, 863 (1982).
[22] E.A. Reinsch, J. Chem. Phys. **83**, 5784 (1985).
[23] D.M. Bishop and B. Lam, Phys. Rev. A **37**, 464 (1988), and references therein.
[24] D.M. Bishop and B. Lam, J. Chem. Phys. **88**, 3398

(1988).
[25] N.K. Rahman, A. Rizzo, and D.L. Yeager, Chem. Phys. Lett. **166**, 565 (1990).
[26] M. Jaszunski and B.O. Roos, Mol. Phys. **52**, 1209 (1984).
[27] S.P.A. Sauer, G.H.F. Dierksen, and J. Oddershede, Int. J. Quantum Chem. **39**, 667 (1991).
[28] J. Rychlewski, Mol. Phys. **41**, 833 (1980).
[29] J. Rychlewski, Chem. Phys. Lett. **73**, 135 (1980).
[30] D.M. Bishop and J. Pipin, Phys. Rev. A **36**, 2171 (1987).
[31] D.M. Bishop and B. Lam, J. Chem. Phys. **89**, 1571 (1988).
[32] D.M. Bishop and J. Pipin, J. Chem. Phys. **94**, 6073 (1991).
[33] D.M. Bishop, J. Pipin, and M. Rérat, J. Chem. Phys. **92**, 1902 (1990).
[34] D.M. Bishop, J. Pipin, and S.M. Cybulski, Phys. Rev. A **43**, 4845 (1991).
[35] F. Maeder and W. Kutzelnigg, Chem. Phys. Lett. **37**, 285 (1976).
[36] W. Meyer, Chem. Phys. **17**, 27 (1976).
[37] A.J. Thakkar, J. Chem. Phys. **75**, 4496 (1981).
[38] R. Luyckx, P. Coulon, and H.N.W. Lekkerkerker, Chem. Phys. Lett. **48**, 187 (1977).
[39] A.D. Buckingham and P.G. Hibbard, Symp. Faraday Soc. **2**, 41 (1968).
[40] P.W. Fowler, P. Jorgensen, and J. Olsen, J. Chem. Phys. **93**, 7256 (1990).
[41] M.A. Matias and J.C. Varandas, Mol. Phys. **70**, 623 (1990).
[42] C. Huiszoon and W.J. Briels (unpublished).
[43] M. Caffarel and P. Claverie, J. Chem. Phys. **88**, 1088 (1988); **88**, 1100 (1988).
[44] M. Caffarel, X. Gadea, and D.M. Ceperley, Europhys. Lett. **16**, 249 (1991).
[45] M. Caffarel and D.M. Ceperley, J. Chem. Phys. **97**, 8415 (1992).
[46] H.B.G. Casimir and D. Polder, Phys. Rev. **73**, 360 (1948).
[47] H. Koch and R.J. Harrison, J. Chem. Phys. **95**, 7479 (1991).
[48] E.L. Pollock and D.M. Ceperley, Phys. Rev. B **30**, 2555 (1984).
[49] D. Gugan and G.W. Michel, Mol. Phys. **39**, 783 (1980).
[50] F.B. Van Duijneveldt, IBM Technical Report No. RJ945 (1971) (unpublished).
[51] G. Chalasinski, S. Van Smaalen, and F.B. van Duijneveldt, Mol. Phys. **45**, 1113 (1982).
[52] P. Siegbahn and B. Liu, J. Chem. Phys. **68**, 2457 (1978).
[53] G. Lamm and A. Szabo, J. Chem. Phys. **72**, 3354 (1980).